

REVIEW OF THE FATIGUE PERFORMANCE OF STAINLESS STEEL 316L PARTS MANUFACTURED BY SELECTIVE LASER MELTING

MENG ZHANG, HUA LI

School of Mechanical and Aerospace Engineering, Nanyang Technological University, 50 Nanyang Avenue, Singapore 639798

XIANG ZHANG

Faculty of Engineering & Computing, Coventry University, Coventry CV1 5FB, United Kingdom

DAVID HARDACRE

*Lloyd's Register EMEA, Energy (Inspection Service Line)
Churchills, Thorncliffe Park Estate, Chapeltown, Sheffield S35 2PH, UK*

ABSTRACT: The powder bed additive manufacturing (AM) process is known to produce defects that can trigger premature fatigue failure under the service loads. Material testing on metallic AM parts thus far has focused on the static mechanical properties, although the fatigue strength is highly pertinent due to the high sensitivity to manufacturing defects. Currently, there is a lack of standardised approaches for the determination of suitable process parameters to ensure consistent acceptable quality of additively manufactured parts. Therefore, this work reviews the formation and prevention of defects in the selective laser melting (SLM) process and examines their impact the quality of stainless steel 316L parts, using the fatigue properties as the main criteria. This will aid future works on the characterisation of material against key process parameters and fatigue tests, and support the development of predictive fatigue models in later phase of the project. Ultimately, the study will contribute to the guidelines for the production and certification of metal AM components and assist manufacturers in achieving required material performance.

KEYWORDS: additive manufacturing; selective laser melting; defects; fatigue performance; steel

REVIEW OF CURRENT WORKS

Mechanisms of defect formation and control for the SLM approach

The laser melting technique, popularly known as SLM, is a powder bed fusion process that achieves material binding through the complete melting/solidification of powdered materials in an enclosed chamber. Fully dense parts approaching 99.9% density can be made with the availability of high power laser and improved processing conditions. Various defects, including pores, cracks, unconsolidated powder, inclusion, poor surface finish and residual stress, may be formed during this process. This project is concerned with any discontinuities that may potentially harm the fatigue properties of a component.

Process-induced defects are common for the SLM process. In descending order of importance, statistical analyses have shown that laser power P , scan speed v , layer thickness t and hatch distance h are the most important parameters during the layer manufacturing process (Casalino *et al.*, 2015; Chatterjee *et al.*, 2003; Yadroitsev *et al.*, 2012). Another parameter, laser spot size d , is less extensively studied as it is fixed by the printer model, but numerical studies have shown that it is of lesser importance (Kamath *et al.*, 2014). A hierarchical design principle was proposed for manufacturing high quality SLM parts (Yadroitsev *et al.*, 2014). Preliminary process parameter

selection should consider the elimination of over and under heating of the metal powder. The use of transient thermal conduction models offer simple and effective prediction of the temperature profile (Contuzzi *et al.*, 2011; Hussein *et al.*, 2013). This should be followed by examination of the manufacturing quality at the single track, single layer and 3D object levels.

In particular, the P - v diagram can be constructed to illustrate the influence of process parameters during single track synthesis, as shown in Figure 1 (based on compiled results from (Gu & Shen, 2009; Laohaprapanon *et al.*, 2012) for 316L). The upper block was obtained for tracks built at a higher layer thickness. It can be seen that insufficient heating results in incomplete melting of the metal powders and potentially lack of fusion pores. Lateral coalescence at low energy input creates large channel-like pores under the surface tension effect (Bauereiß *et al.*, 2014; Morgan *et al.*, 2004). Excessive heating leads to material evaporation and melt pool instability where high recoil pressure and the Marangoni flow could be activated. Spattering, similar to that in laser welding, may be incurred (Liu *et al.*, 2015; Simonelli *et al.*, 2015). Vortices induced beneath the melt pool surface can cause bubbles to cluster at the melt pool centre (Dai & Gu, 2014). In addition, keyhole melting and balling have to be avoided as they generate large irregular pores that significantly compromise material strength. The occurrence of these two phenomena may be quantitatively deduced from their respective melt pool dimensions (King *et al.*, 2014).

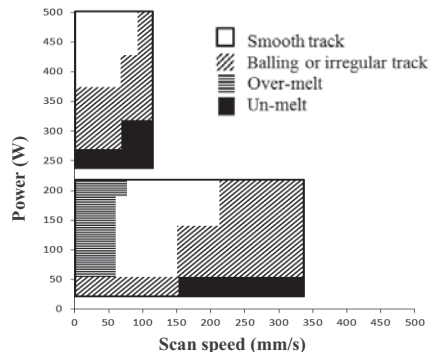


Figure 1. The P - v process map

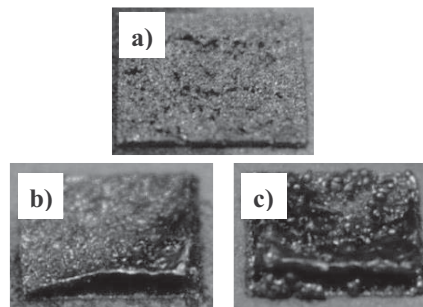


Figure 2. Parts (side lengths of 1 cm) showing a) incomplete melting, b) warping, and c) balling.

Multi-track and multi-layer consolidation produces 3D components. Track overlapping ensures sufficient bonding between adjacent tracks and layers. However, the relationships between porosity and process parameters are not linear even within this domain. Powder denudation can cause reduction of the consolidation zone, resulting in lower depth at part interior than the edges (Yadroitsev & Smurov, 2011). To compensate for this, a large h value should be used, contrary to conventional belief that small h allows for more effective track overlapping. Figure 2 shows parts obtained in this study due to the selection of inappropriate process conditions. The cumulative effect of layerwise building can be seen in Figure 2b, where a slight edge curling had resulted in significant distortion and overheating during the subsequent fabrication steps and the formation of coarse balls (Figure 2c).

Other factors, such as powder quality, e.g. size and shape distributions and contaminants, can aggravate the stochastic nature of the process, thus reducing its controllability. Scanning strategies, e.g. rotational scanning, island scanning and remelting, can also be adopted to eliminate pores. Platform preheating is an effective strategy for relieving stress and preventing crack formation.

Characterisation of defects formed during the SLM process

Detection of defects by the non-destructive X-ray computed tomography (XCT) technique has shed light on the characteristic discontinuities formed by the SLM approach, allowing statistical descriptions of the defect properties. XCT studies performed on 316L parts revealed that the highest pore counts are obtained when parts are built parallel to the platform, with an average size of 300 to 600 μm and sphericity factor of 0.6 (Ziółkowski *et al.*, 2014). Pores tend to be elongated in the plane of the deposition layer and bigger pores were found towards the specimen centre rather than the surface due to higher solidification rate at the centre (Spierings *et al.*, 2011).

The use of microscopic method for porosity examination is common. Larger deviations in density measurements were observed with incomplete melting or balling, which give rise to irregular voids and compromise the measurement accuracy (Spierings *et al.*, 2011). Stereological corrections are effective means for reconstructing 3D porosity from 2D results (Williams *et al.*, 2015).

Microstructure and fatigue properties relationship

Influence of defects on fatigue properties

Fatigue properties are sensitive to defects. It was observed that fatigue strength reduces with higher porosity content and the presence of pores promotes interdendritic crack propagation due to higher crack driving force (Kim *et al.*, 2011). The presence of a larger number of defects implies a higher possibility for crack initiation, resulting in inferior fatigue performance at the macro-scale.

Considering a crack-like defect as the crack initiation site, crack propagation dominates fatigue life and the influence on fatigue limit σ_{lim} of metal alloys was derived empirically from the definition of the threshold stress intensity factor range as (Murakami, 1994):

$$\sigma_{\text{lim}} = \frac{C(H_v+120)}{(\sqrt{\text{area}})^{1/6}} \quad (1)$$

The effect of defect geometry is accounted for by the projected area $\sqrt{\text{area}}$ of the critical defect on a plane and that of defect location by the correction factor C . It is to be noted that microstructural features are not well accounted for by this equation. The application of the theories of Linear Elastic Fracture Mechanics (LEFM) forms the basis of many fatigue prediction models.

In the case where the short crack problem is relevant, modifications to LEFM may need to be made. According to El Haddad *et al.*, the critical size of the short fatigue crack can be predicted by

$$a_0 = \frac{1}{\pi} \left(\frac{\Delta K_{\text{th}}}{\sigma_{\text{lim}}} \right)^2 \quad (2)$$

For SLM-processed 316L components, a_0 is approximated to be 70 μm for HIPed (hot isostatic press) condition and 250 μm for as-built condition based on values obtained in (Riemer *et al.*, 2014). Alternatively, ASTM specifications state that a crack is considered short if the plastic zone size is greater than $a_0/50$ (Hussain, 1997). The impact of defect size on fatigue strength can be represented by the Kitagawa–Takahashi (K-T) diagram, as shown in Figure 3.

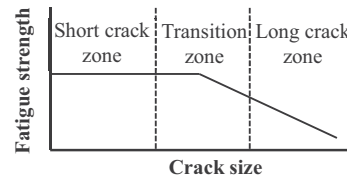


Figure 3. The effect of crack size is illustrated by the K-T diagram.

However, the applicability of existing models developed for the isotropic materials to SLM components is questionable, as the SLM process is associated with high defect density where interaction among the micro-scale pores is possible and the material is anisotropic. Studies aimed at applying the LEFM to fatigue strength prediction of Ti alloys show that modifications need to be made for parts in the as-built and HIPed conditions (Leuders *et al.*, 2015). No published work is known for the 316L material.

Competition between microstructure and defect

As indicated by the high elongation at break (Riemer *et al.*, 2014), austenitic 316L is a highly ductile material due to the absence of phase transformation under cooling. This may reduce the local stress at defects and delay the onset of crack initiation. In the same study and in (Spierings *et al.*, 2013), the fatigue strength of SLM parts without post-processing treatment was comparable with conventional 316L parts, alluding to the possibility that this material is not porosity-sensitive in terms of its fatigue properties. In fact, microstructural features, e.g. grain size, shape and texture, may be more important. Gains homogenisation through recrystallization induced by HIP gives better fatigue property and coarse-grained materials are more resistant to fatigue crack initiation (Radhakrishnan & Mutoh, 2013). Besides, due to the high ductility, residual stress (Riemer *et al.*, 2014) and surface roughness (Spierings *et al.*, 2013) were found to play insignificant roles.

In addition, the stress-dependency of fatigue failure cannot be neglected. Within the low cycle fatigue regime, fatigue damage is dominated by the propagation phase and persistent slip bands appear to be the main initiation sites (Murakami, 2002), despite the presence of larger pores. Results from (Leuders *et al.*, 2014) seem to support this observation for SLM-processed 316L parts. Finite element modelling of this material also shows that whether a pre-existing defect triggers crack initiation depends on the cycle regime (Sistaninia & Niffenegger, 2015).

Another relevant feature could be the grain structure in the melt pool, characterised by fine grains at the melt pool centre, coarse grains in heat affected zone towards the boundary (Thijs *et al.*, 2013). This partly resembles the microstructure in welded parts, where grain size around the initiating defect affects the damage propagation rate (Pickard *et al.*, 1975).

Probabilistic model for fatigue property prediction

Defect distributions have been utilised for the prediction of the scatter in fatigue data. In general, potential sources of uncertainties include defects, i.e. size, number, location and shape, microstructures and mechanical properties. Failure criteria need to be defined and the respective failure probabilities can then be evaluated. For example, in (Pessard *et al.*, 2013), the equivalent stress and the threshold stress intensity range were represented statistically for simulating different regions of the K-T diagram. A similar approach was adopted in (Koutiri *et al.*, 2013), though with the use of different failure criteria. Estimations are often made based on the weakest-link theory.

Depending on the modelling approach, explicit expressions of failure probabilities could be difficult to obtain in reality. The Monte-Carlo simulation is sometimes adopted. The input domain, which may refer to descriptors of the defect population, has to be defined. Fatigue samples have to be generated based on the input distribution and the outputs, e.g. fatigue strength, will be computed using deterministic models. In simplified cases, the Monte-Carlo simulation can be avoided by directly linking the defect size distribution with fatigue life (Charkaluk *et al.*, 2014).

SUMMARY

Literature survey has shown that:

- Defects are prevalent in SLM parts and can be controlled by process parameter selection.
- The fatigue property of austenitic 316L is affected by manufacturing defects as well as the microstructure, depending on the life regimes.
- Owing to the high ductility, 316L shows defect-tolerant fatigue behaviour in comparison with other AM-built alloys.
- It is pertinent to examine the interaction of microstructure and defect, perhaps through different post-processing treatments, for the development of fatigue prediction models using both the deterministic and probabilistic approaches.

REFERENCES

- Bauereiß, A., Scharowsky, T., & Körner, C. (2014). Defect generation and propagation mechanism during additive manufacturing by selective beam melting. *J Mater Process Technol*, 214(11), 2522-2528.
- Casalino, G., Campanelli, S., Contuzzi, N., & Ludovico, A. (2015). Experimental investigation and statistical optimisation of the selective laser melting process of a maraging steel. *Opt Laser Technol*, 65, 151-158.
- Charkaluk, E., Constantinescu, A., Szymtka, F., & Tabibian, S. (2014). Probability density functions: from porosities to fatigue lifetime. *Int J Fatigue*, 63, 127-136.
- Chatterjee, A., Kumar, S., Saha, P., Mishra, P., & Choudhury, A. R. (2003). An experimental design approach to selective laser sintering of low carbon steel. *J Mater Process Technol*, 136(1), 151-157.
- Contuzzi, N., Campanelli, S., & Ludovico, A. (2011). 3D finite element analysis in the selective laser melting process. *Int J Simul Model*, 10(3), 113-121.
- Dai, D., & Gu, D. (2014). Thermal behavior and densification mechanism during selective laser melting of copper matrix composites: Simulation and experiments. *Mater Des*, 55, 482-491.
- Gu, D., & Shen, Y. (2009). Balling phenomena in direct laser sintering of stainless steel powder: Metallurgical mechanisms and control methods. *Mater Des*, 30(8), 2903-2910.
- Hussain, K. (1997). Short fatigue crack behaviour and analytical models: a review. *Eng Fract Mech*, 58(4), 327-354.
- Hussein, A., Hao, L., Yan, C., & Everson, R. (2013). Finite element simulation of the temperature and stress fields in single layers built without-support in selective laser melting. *Mater Des*, 52, 638-647.
- Kamath, C., El-dasher, B., Gallegos, G. F., King, W. E., & Sisto, A. (2014). Density of additively-manufactured, 316L SS parts using laser powder-bed fusion at powers up to 400 W. *Int J Adv Manuf Tech*, 74(1-4), 65-78.
- Kim, K., Park, J., Yim, C., & Lee, K. (2011). Effect of porosity on the high cycle fatigue behavior of casing AM60B magnesium alloy. *Procedia Eng*, 10, 165-170.
- King, W. E., Barth, H. D., Castillo, V. M., Gallegos, G. F., Gibbs, J. W., Hahn, D. E., . . . Rubenchik, A. M. (2014). Observation of keyhole-mode laser melting in laser powder-bed fusion additive manufacturing. *J Mater Process Technol*, 214(12), 2915-2925.
- Koutiri, I., Bellett, D., Morel, F., & Pessard, E. (2013). A probabilistic model for the high cycle fatigue behaviour of cast aluminium alloys subject to complex loads. *Int J Fatigue*, 47, 137-147.
- Laohaprapanon, A., Jeamwathanachai, P., Wongcumchang, M., Chantarapanich, N., Chantaweroad, S., Sitthiseripratip, K., & Wisutmethangoon, S. (2012). *Optimal scanning condition of selective laser melting processing with stainless steel 316l powder*. Paper presented at the Advanced Materials Research.

- Leuders, S., Lieneske, T., Lammers, S., Tröster, T., & Niendorf, T. (2014). On the fatigue properties of metals manufactured by selective laser melting—The role of ductility. *J Mater Res*, 29(17), 1911-1919.
- Leuders, S., Vollmer, M., Brenne, F., Tröster, T., & Niendorf, T. (2015). Fatigue Strength Prediction for Titanium Alloy TiAl6V4 Manufactured by Selective Laser Melting. *Metall Mater Trans A*, 1-8.
- Liu, Y., Yang, Y., Mai, S., Wang, D., & Song, C. (2015). Investigation into spatter behavior during selective laser melting of AISI 316L stainless steel powder. *Mater Des*, 87, 797-806.
- Morgan, R., Sutcliffe, C., & O'Neill, W. (2004). Density analysis of direct metal laser re-melted 316L stainless steel cubic primitives. *J Mater Sci*, 39(4), 1195-1205.
- Murakami, Y. (1994). Inclusion rating by statistics of extreme values and its application to fatigue strength prediction and quality control of materials. *J Res Natl Inst Stan*, 99, 345-345.
- Murakami, Y. (2002). *Metal fatigue: effects of small defects and nonmetallic inclusions*. Elsevier.
- Pessard, E., Bellett, D., Morel, F., & Koutiri, I. (2013). A mechanistic approach to the Kitagawa–Takahashi diagram using a multiaxial probabilistic framework. *Eng Fract Mech*, 109, 89-104.
- Pickard, A., Ritchie, R., & Knott, J. (1975). Fatigue crack propagation in a type 316 stainless steel weldment. *Met Technol*, 2(1), 253-263.
- Radhakrishnan, V., & Mutoh, Y. (2013). *On fatigue crack growth in stage I*. Proceedings of the EGF1 Conference.
- Riemer, A., Leuders, S., Thöne, M., Richard, H., Tröster, T., & Niendorf, T. (2014). On the fatigue crack growth behavior in 316L stainless steel manufactured by selective laser melting. *Eng Fract Mech*, 120, 15-25.
- Simonelli, M., Tuck, C., Aboulkhair, N. T., Maskery, I., Ashcroft, I., Wildman, R. D., & Hague, R. (2015). A Study on the Laser Spatter and the Oxidation Reactions During Selective Laser Melting of 316L Stainless Steel, Al-Si10-Mg, and Ti-6Al-4V. *Metall Mater Trans A*, 1-10.
- Sistaninia, M., & Niffenegger, M. (2015). Fatigue crack initiation and crystallographic growth in 316L stainless steel. *Int J Fatigue*, 70, 163-170.
- Spierings, A., Schneider, M., & Eggenberger, R. (2011). Comparison of density measurement techniques for additive manufactured metallic parts. *Rapid Prototyping J*, 17(5), 380-386.
- Spierings, A., Starr, T., & Wegener, K. (2013). Fatigue performance of additive manufactured metallic parts. *Rapid Prototyping J*, 19(2), 88-94.
- Tammas-Williams, S., Zhao, H., Léonard, F., Derguti, F., Todd, I., & Prangnell, P. (2015). XCT analysis of the influence of melt strategies on defect population in Ti-6Al-4V components manufactured by Selective Electron Beam Melting. *Mater Charact*, 102, 47-61.
- Thijs, L., Kempen, K., Kruth, J.-P., & Van Humbeeck, J. (2013). Fine-structured aluminium products with controllable texture by selective laser melting of pre-alloyed AlSi10Mg powder. *Acta Mater*, 61(5), 1809-1819.
- Yadroitsev, I., Krakhmalev, P., & Yadroitsava, I. (2014). Hierarchical design principles of selective laser melting for high quality metallic objects. *Additive Manufacturing*.
- Yadroitsev, I., & Smurov, I. (2011). Surface morphology in selective laser melting of metal powders. *Phys Procedia*, 12, 264-270.
- Yadroitsev, I., Yadroitsava, I., Bertrand, P., & Smurov, I. (2012). Factor analysis of selective laser melting process parameters and geometrical characteristics of synthesized single tracks. *Rapid Prototyping J*, 18(3), 201-208.
- Ziółkowski, G., Chlebus, E., Szymczyk, P., & Kurzac, J. (2014). Application of X-ray CT method for discontinuity and porosity detection in 316L stainless steel parts produced with SLM technology. *Arch Civ Mech Eng*, 14(4), 608-614.